PAPER • **OPEN ACCESS**

Analysis of columnar-to-equiaxed transition experiment in lab scale steel casting by a multiphase model

To cite this article: S. Sachi *et al* 2019 *IOP Conf. Ser.: Mater. Sci. Eng.* **529** 012039

IOP Conf. Series: Materials Science and Engineering **529** (2019) 012039 doi:10.1088/1757-899X/529/1/012039

Analysis of columnar-to-equiaxed transition experiment in lab scale steel casting by a multiphase model

S. Sachi[1], M. Založnik[1], H. Combeau[1], Ch.-A. Gandin[2], M. Gennesson[3], J. Demurger[3], M. Stoltz[3] and I. Poitrault[4]

[1] Université de Lorraine, CNRS, IJL, F-54000 Nancy, France
[2] MINES ParisTech, CEMEF UMR CNRS 7635, F-06904 Sophia, Antipolis, France
[3] Ascométal CREAS, Avenue de France, BP 70045, 57301, Hagondange, France
[4] ArcelorMittal Industeel, 71201 Le Creusot, France

E-mail: savya.sachi@univ-lorraine.fr

Abstract.

Correct prediction of composition heterogeneities and grain structure across a steel ingot is critical in optimizing the industrial processing parameters for enhanced performance. The columnar to equiaxed transtion (CET) is a microstructural transition which is strictly controlled as it affects the mechanical properties of the final product along with the macrosegregation patterns. Larger equiaxed regions are preferred for most industrial applications. CET is significantly affected by the number density of equiaxed grains and by the nucleation undercooling. 8 kg 42CrMo4 alloy steel ingots (240 mm x 60 mm x 60 mm) were cast. The cast structure was characterized by ASCOMETAL. The experiments were simulated with a process-scale model of solidification that incorporates a multiscale description of the microstructure formation. The goal of the present study is to show the capabilities of such a process-scale solidification model to explain the observed structure distributions (extent of the columnar and equiaxed zones, equiaxed-to-columnar transition).

1. Introduction

Solidification processing is one of the most important routes to produce metals and alloys. During solidification, parameters such as the temperature gradient and the growth rate which are dependent on the casting practice and on alloy properties, result in a wide variety of microstructures and material behaviour. Solidification results in two types of grain morphologies: columnar and equiaxed. Nucleation of crystals in an undercooled melt results in equiaxed grains whereas columnar grains form when the heat flux is unidirectionally oriented. Transition from columnar to equiaxed growth is called Columnar-to-equiaxed (CET) transition and occurs when nucleation of equiaxed grains occurs ahead of the columnar front. CET is significantly affected by the number density of the equiaxed grains. The nuclei which subsequently evolve into equiaxed grains are introduced through heterogeneous nucleation or dendrite fragmentation. Heterogeneous nucleation can occur during any time of solidification due to constitutional supercooling. Dendrite fragmentation can occur due to convection or fallout from the upper surface of the ingot.

Numerical simulations have demonstrated that density of grains in the melt can affect the intensity of macrosegregation [1, 2, 3]. Deposition of the solute depleted grains along with the rejection of solute into the liquid is the primary cause of macrosegregation. The grain size and the morphology (dendritic or globular) determine the settling dynamics of the equiaxed grains. The size and the morphology of the deposited equiaxed grains further affects the permeability of the deposited layer, thus influencing the permeation of solute rich liquid through the packed layers. Globular grains lead to more pronounced macrosegregation than dendritic grains. It has further been observed that segregation can also result in "solutal blocking" of the columnar front and result in CET [4]. Thus, the final microstructure obtained after casting is a result of multitude of physical phenomena occurring simultaneously. In this work, the influence of origins of the equiaxed grains on the CET in a small steel casting has been investigated.

2. Model description

The multiscale multiphase model of solidification SOLID is used for this study. It is based on the volume averaging method with three hydrodynamic phases: the solid phase and two liquid phases (interdendritic and extradendritic) [5]. The present version is an extension of the two phase model [1, 6] and models the growth of the columnar grains along with the development of moving equiaxed grains [2, 7]. The morphology of the equiaxed grains in the volume averaged model is based on the idea of dendrite envelope as proposed by Rappaz and Thevoz [8]. The model distinguishes between the liquid outside the envelope (extradendritic liquid) and the liquid inside the envelope (interdendritic liquid) which is assumed to be homogeneous. Same envelope shape and morphological parameters are used to model the columnar and equiaxed structure. A columnar grain is schematized as an assembly of equiaxed grains arranged on a cubic sublattice with a volume density of substructures distinct from that of equiaxed grains [2]. Columnar grains originate at the mold wall and the growth direction is aligned with the local thermal gradient ahead of the front. The columnar front is tracked using a method developed by Ludwig and Wu [9]. Equiaxed grains originate from dendrite fragments or heterogeneous nuclei. The growth of the columnar and equiaxed grains envelopes are calculated according to the LGK model [10]. In the present model, a mixed zone containing columnar and equiaxed grains is considered in the vicinity of the columnar tips. In this zone, the system contains six phases, three phases associated with the equiaxed grains and three phases associated with the columnar grains.

The model contains two parts: a) macroscopic transport model which accounts for the momentum, mass, heat, solute mass and grain populations conservation b) microscopic growth model which accounts for the nucleation and growth of the grains. The two parts of the model are coupled using an operator splitting scheme [6]. The motion of the liquid melt and the solid grains at the macroscopic scale are modeled by taking into account: inertial forces, drag forces at the solid-liquid interface and the buoyancy forces. The buoyancy forces are induced by liquid density variation (thermosolutal convection modeled with Boussinesq approximation) and density difference between liquid and solid. Heterogeneous nucleation of equiaxed grains is modeled using an instantaneous nucleation law. Multiple sets of heterogeneous nucleation sites (nuclei) are used, each set is described by a distinct nucleation undercooling and a population density. Columnar dendrite fragments are a second source of new equiaxed grains. They are introduced ahead of the columnar front at a predefined rate when the local thermal gradient drops below a critical value. Once nucleation occurs, equiaxed grains grow as dispersed solid phases and freely move. They are introduced as globular grains with a diameter of 1 μm. The population balance for grains and nuclei are accounted for. While the grains move with the solid velocity, the nuclei move along with the liquid. When the envelope fraction of the equiaxed grains is above the packing fraction, solid phase is considered stationary and the flow regime changes from a slurry flow to a porous flow. Two phenomena responsible for CET are

considered:"mechanical blocking" and "solutal blocking". "Mechanical blocking" occurs when the equiaxed grain fraction in the mixed zone reaches a critical value which can range from 0.2 [11] to 1. In the present work, the mechanical blocking fraction is set to 0.5 according to the criterion proposed by Hunt [12]. "Solutal blocking" occurs when the chemical undercooling reduces sufficiently to prevent the growth of the columnar front, effectively blocking it [4]. "Equiaxed-to-Columnar" (ECT) transition, which is observed at the top of industrial steel ingots [3], is also modeled.

3. Experimental setup, observations and simulation setup

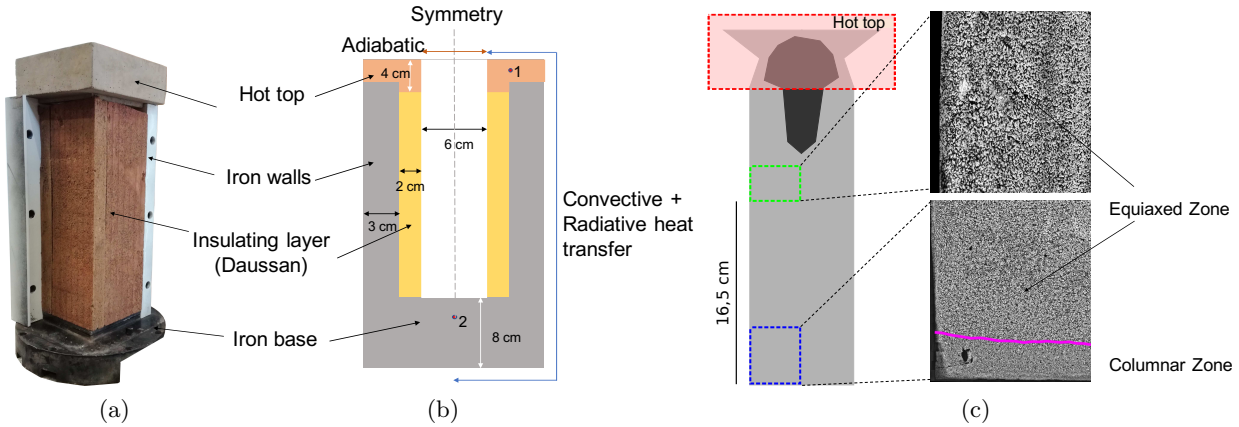

Figure 1. (a) Experimental setup used for the ingot casting with two of the iron walls have been disassembled to reveal the added insulation layer in the mold and (b) geometry used for the simulations. The red dots show the positions of the thermocouples 1 and 2 respectively (c) Diagram showing the etched locations along with the associated microstructure

8 kg Experimental trials were conducted by Ascométal to see the effect of inoculants on the cast structure. The composition of the 42CrMo4 steel is 0.4 wt% C, 0.2 wt% Si, 0.7 wt% Mn, 0.3 wt% Mo and 1.1 wt% Cr. The ingots have a square cross section as shown in Fig 1a. The hot top is a composite material with a chemical composition of 45% Al_2O_3 - 44 % SiO_2 - 5 % Fe_2O_3 - 6% binders. The walls of the mold have been insulated from the inside with a fibrous composite produced by Daussan France (Woippy, France). Its chemical composition is 83% SiO_2 - 2% Al_2O_3 - 2% CaO - 13 % binders. This setup promotes directional solidification from the bottom. The metal to be cast is heated to 1560 °C after which it is poured into the preheated mold. The experiments were instrumented using thermocouples. Macroetching were performed on the entire surface of the ingot. Fig. 1c shows a ≈1.5 cm thick columnar zone at the bottom for a cast ingot with no inoculating agent additions. No columnar zone was observed along the vertical walls of the casting. A structural gradient can be observed between the edge and the center of the sample. A coarser structure is observed in the top and a much finer structure is observed in the bottom.

We consider a simplified 2D axis-symmetric geometry as shown in Fig 1b. The numerical domain was discretized into approximately 1700 cells with an average cell of 4 mm. The time step varies from 5×10^{-3} to 0.01 seconds. The thermo-physical parameters used for the simulations are listed in Table 1. To model the steel, we consider a binary iron-carbon alloy with a nominal composition of C_0=0.4 wt.% and neglecting the other alloying additions. This is because carbon has the strongest effect on the solidification path and the solutal buoyancy. The experimental temperature measurements in the mold were used to fit the thermal boundary conditions and to set the initial temperature of the mold components. An external temperature of 200 °C was

used. The filling stage has been neglected and the initial temperature and carbon concentration fields in the steel are assumed to be uniform.

Table 1. Thermophysical properties used in the simulations.

Property	**Symbol**	**Units**	**Value**
Nominal carbon concentration	C_0	$[\%mass]$	0.4
Partition coefficient	k_p	$[-]$	0.18
Melting point of the pure substance	T_f	$[°C]$	1538
Liquidus slope	m_l	$[°C/\%mass]$	-85
Liquidus temp. at C_0	$T_{liq}\,(C_0)$	$[°C]$	1504
Reference density	ρ	$[kg/m^3]$	7040
Solutal expansion coeff.	β_C	$[\%mass^{-1}]$	1.4×10^{-2}
Thermal expansion coeff.	β_T	$[K^{-1}]$	1.7×10^{-4}
Latent heat	L_f	$[J/kg]$	3.09×10^5
Thermal conductivity	k	$[W/(mK)]$	30
Heat capacity	C_p	$[J/(Kkg)]$	500
Kinematic viscosity	ν_l	$[kg/(ms)]$	4×10^{-3}
Diffusion coefficient	L_f	$[m^2 s]$	3×10^{-9}

4. Results and discussion

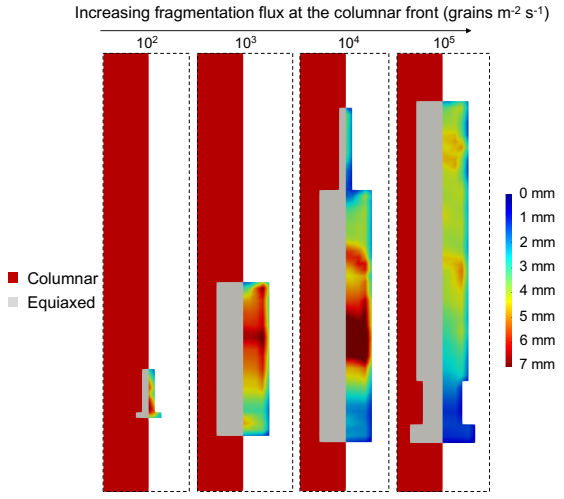

Figure 2. Predicted structure and grain size distribution for fragmentation rates 10^2, 10^3, 10^4 and 10^5 $m^{-2}s^{-1}$. Left hand section shows the grain structure (equiaxed and columnar) and the right half shows the grain size only for the equiaxed regions

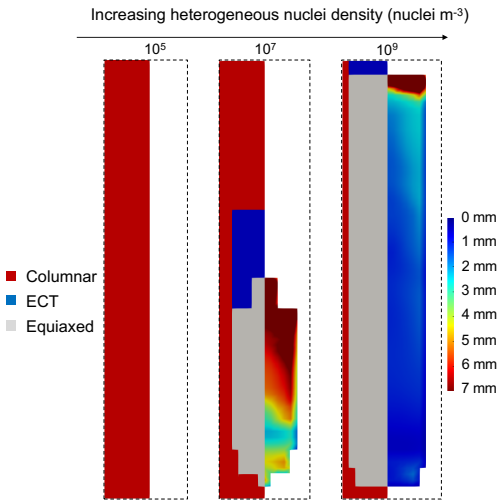

Figure 3. Predicted structure and grain size distribution for heterogeneous nuclei density of 10^5, 10^7 and 10^9 m^{-3}

The simulation results matched with the experimental thermocouple measurements which validated the thermal boundary conditions being used. We use the software SOLID to investigate the structure obtained for the above experimental setup. The simulations investigated the two scenarios of equiaxed grain formation and the impact on CET:

(i) Only fragmentation of columnar dendrites with no heterogeneous nucleation
(ii) Only heterogeneous nuclei with no fragmentation of the columnar dendrites

In all cases, solidification starts with the formation of the columnar dendrites. Simulations with only fragmentation are shown in Fig. 2. Fluxes of fragments across the columnar front, ϕ_0 (nuclei. $m^{-2}s^{-1}$), of 10^2, 10^3, 10^4 and 10^5 are used. The fragments are introduced in the liquid adjacent to the columnar front. Equiaxed grains start to form from the fragments in front of the columnar zone. Initially the equiaxed grains are small and move along with the liquid. At around 40-50 seconds, the grains start sedimenting. The columnar front is blocked first at the bottom and then further up in the ingot. Lower fragmentation rates results in delayed blocking of the columnar front. As the equiaxed grains descend, they are blocked when the grain envelope fraction (g_{env}) reaches 0.3. The first grains that settle to the bottom are small and globular. As solidification progresses upwards, the equiaxed morphology changes to dendritic and the grain size increases. Lower fragmentation rates results in larger grain size towards the top part of the equiaxed region. Fragmentation rate of 10^5 nuclei. $m^{-2}s^{-1}$ gives a satisfactory fit with the experimentally observed observed grain size at the bottom. However, it fails to produce the observed thickness of the columnar zone at the bottom and the size evolution of the equiaxed grains along the height of the cast structure. It can be concluded that fragmentation alone cannot reproduce the observations.

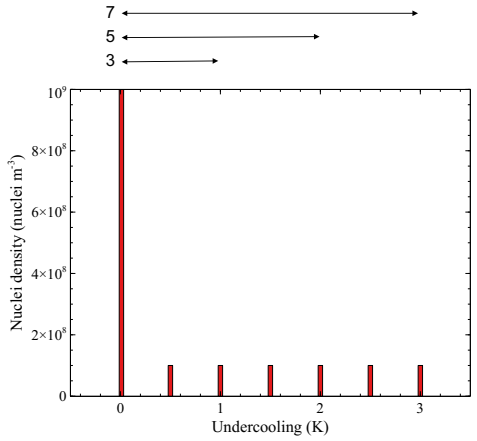

Figure 4. Discretization of nucleation sites with respect to critical undercooling

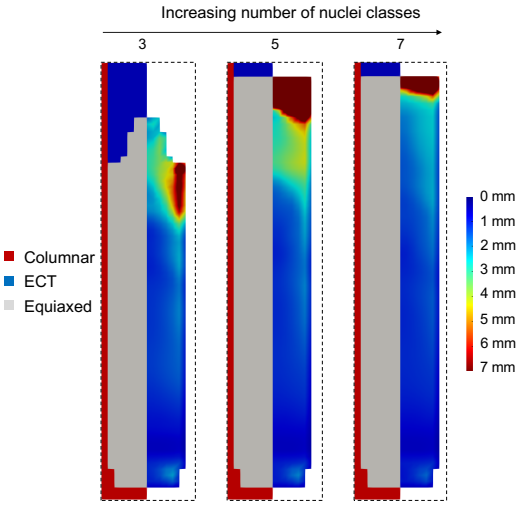

Figure 5. Predicted structure and grain size distribution for heterogeneous nuclei density of 10^9 m^{-3} with varying number of nuclei classes

Fig. 3 shows the results for the heterogeneous nucleation of equiaxed grains without fragmentation. The heterogeneous nucleation simulates the effect of inoculants as well as the possible grains detached from the mold surface during filling. Multiple classes of nuclei as shown in Fig. 4 are used for the next shown simulations [13]. Solidification starts with the formation of the columnar front on the bottom and the development of fluid flow due to thermal convection. The liquid convection results in the ingot being undercooled and all the nuclei are activated. The highest undercooling is obtained in the vicinity of the columnar front at the bottom and the liquid flow drives the liquid to the bottom. This favours the growth of the equiaxed grains which sediment to the bottom of the ingot and block the growth of the columnar front. No equiaxed zone is obtained for a nuclei density of 10^5 nuclei. m^{-3}. Nuclei density of 10^9 nuclei.

m^{-3} produces a completely equiaxed structure with fine columnar zone of 0.4 mm thickness along the vertical walls. The thickness of the columnar zone on the bottom is 0.8 cm and the grain size is in the range of 1-2 mm. Experimental observations are reproduced except for the coarse grain size at the top. Once all the equiaxed grains have sedimented, the columnar structure is free to develop in the remaining liquid which results in an ECT occurring at the top of the sedimented equiaxed grains. Further,the columnar structure originating from ECT can meet the columnar front originating from the mold as can be seen for volumetric injection rate of 10^7 nuclei. m^{-3} in Fig. 3. Fig. 5 shows the influence of number of nuclei classes on the structure and the grain size. For simulations with 3 classes, nuclei were activated at an undercooling of 0, 0.5 and 1 K while for 5 classes, nuclei were activated at an undercooling of 0, 0.5, 1, 1.5 and 2 K. Using multiple classes of heterogeneous nuclei delays the formation of ECT as can be seen in Fig. 5. The size classes used for the simulations is shown in Fig. 4. Nucleation sites requiring large undercooling for activation are introduced towards the later stages of solidification when the liquid fraction is small. The equiaxed grains obtained from these nuclei prevent the growth of the columnar grains unless they sediment and allow an ECT transition. As these nuclei are injected in a highly undercooled liquid, coarse equiaxed grains are obtained at the top as is observed in Fig. 5.

5. Conclusions

Simulations were carried out for 8 kg steel ingot cast by Ascométal. Different origins of equiaxed grains: injection of fragments into the liquid ahead of the columnar front and classical heterogeneous nucleation were simulated using SOLID. A parametric study of the fragmentation shows that this mechanism cannot accurately predict the experimental CET. The top of the structure exhibits a purely columnar structure which is not observed experimentally and the grain size obtained was larger than what was experimentally observed. Heterogeneous nucleations were incorporated. A single class of nuclei resulted in the top region being depleted of the grains and resulted in CET transition. Thus, multiple nuclei classes were incorporated which seems to match better with the experimental observations. Further work is required to understand the mechanism better and the effect of solidification path on this phenomena.

Acknowledgements

This work was supported by Ascométal Creas, ArcelorMittal Industeel Creusot, Aubert & Duval, Aperam Alloys, Transvalor, Sciences Computers Consultants, Affival and IXTREM in the framework of the FUI SOFT-DEFIS project.

References

[1] Combeau H, Založnik M, Hans S and Richy P E 2009 *Metall. Mater. Trans. B* **40** 289–304
[2] Leriche N 2015 *Etude de la Transition Colonnaire-Equiaxe dans les lingots et en coulée continue d'acier et influence du mouvement des grains* Ph.D. thesis University of Lorraine
[3] Kumar A, Založnik M, Combeau H, Demurger J and Wendenbaum J 2012 *International conference on ingot casting, rolling and forging, Aachen, Germany*
[4] Martorano M A, Beckermann C and Gandin C A 2003 *Metall. Mater. Trans. A* **34** 1657–1674
[5] Tveito K O, Pakanati A, MHamdi M, Combeau H and Založnik M 2018 *Metall. Mater. Trans. A* **49** 2778–2794
[6] Založnik M and Combeau H 2010 *Comput. Mater. Sci.* **48** 1 – 10
[7] Leriche N, Combeau H, Gandin C A and Založnik M 2015 *IOP Conference Series: Mater. Sci. Eng.* vol 84
[8] Rappaz M and Thevoz P 1987 *Acta Metallurgica* **35** 1487–1497
[9] Ludwig A and Wu M 2005 *Mater. Sci. Eng. A* **413** 109–114
[10] Lipton J, Glicksman M and Kurz W 1984 *Mater. Sci. Eng.* **65** 57–63
[11] Biscuola V and Martorano M 2008 *Metall. Mater. Trans. A* **39** 2885–2895
[12] Hunt J 1984 *Mater. Sci. Eng.* **65** 75–83
[13] Heyvaert L, Bedel M, Založnik M and Combeau H 2017 *Metallurgical and Materials Transactions A* **48** 4713–4734